ACS APPLIED BIO MATERIALS Cite This: ACS Appl. Bio Mater. 2018, 1, 756−767 Article www.acsabm.org

Influence of Charge on Hemocompatibility and Immunoreactivity of Polymeric Nanoparticles

Liyu Chen,[†,‡,§] Joshua J. Glass,[∥,⊥] Robert De Rose,[∥,#] Claudia Sperling,[△] Stephen J. Kent,[∥,⊥,○] Zachary H. Houston,[†,‡,§] Nicholas L. Fletcher,[†,‡,§] Barbara E. Rolfe,[*,†] and Kristofer J. Thurecht[*,†,‡,§]

[†]Australian Institute for Bioengineering and Nanotechnology (AIBN), [‡]Centre for Advanced Imaging, and [§]ARC Centre of Excellence in Convergent BioNano Science and Technology, The University of Queensland, Brisbane, Queensland 4072, Australia

[∥]ARC Centre of Excellence in Convergent Bio-Nano Science and Technology, The University of Melbourne, Melbourne, Australia

[⊥]Department of Microbiology and Immunology, Peter Doherty Institute for Infection and Immunity, The University of Melbourne, Melbourne, Victoria 3000, Australia

[#]ARC Centre of Excellence in Convergent BioNano Science and Technology, Monash University, Melbourne, Victoria 3800, Australia

[○]Melbourne Sexual Health Centre and Department of Infectious Diseases, Alfred Health, Central Clinical School, Monash University, Melbourne, Victoria 3800, Australia

[△]Institute Biofunctional Polymer Materials, Max Bergmann Center of Biomaterials, Leibniz-Institut für Polymerforschung Dresden e.V., Dresden D-01069, Germany

Supporting Information

ABSTRACT: The benefits of nanomedicine may be restricted by hemocompatibility and immunoreactivity problems arising from administration of exogenous materials into the bloodstream. To understand how surface charge influences the interaction of polymeric nanoparticles with blood components, we synthesized three well-defined, charge-varied hyperbranched polymers (HBPs) of similar size and analyzed both hemocompatibility and immunoreactivity of these methacrylate-based HBPs ex vivo using primary human blood cell assays and image analyses following intravenous injection into mice. The results show that, regardless of charge, endotoxin-free HBPs had minimal effects on coagulation, platelet, complement, or T cell activation. However, high concentrations (100 μg mL^{-1}) of cationic HBPs led to significant dendritic cell activation, suggesting the potential application of these nanoparticles as vaccine adjuvants to aid efficient antigen presentation. Biodistribution studies showed that intravenously administered charge-neutral HBPs had a longer retention time in the circulation than cationic or anionic HBPs; whereas these neutral HBPs were eventually cleared in the urine, charged HBPs mainly accumulated in liver and spleen. Overall, these results demonstrate that, regardless of surface charge, HBPs display a high level of hemocompatibility. In contrast, immunoreactivity and biodistribution are significantly influenced by charge. Manipulation of surface charge may thus be a useful method by which nanomaterials such as HBPs can be tailored to different clinical applications.

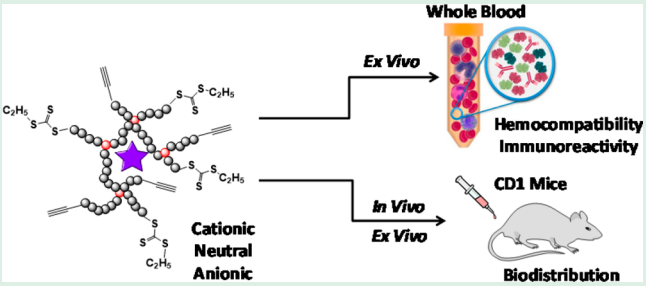

KEYWORDS: *nanomaterials, immune response, hemocompatibility, branched polymer, nanomedicines*

INTRODUCTION

Nanomedicine-based strategies promise to revolutionize the diagnosis and treatment of diseases such as cancer and vascular disease.[1] Nanoconstructs such as liposomes, dendrimers, and nanocrystals are already on the market as clinically approved therapeutics, with many more in the pharmaceutical pipeline (clinical trials or preclinical development).[2] To date, the development of nanoparticles for biomedical application has mainly focused on two key aspects: (1) fabrication of nanostructures to carry moieties (such as therapeutic drugs, targeting ligands, or imaging agents) that facilitate a specific function, and/or (2) the mechanisms responsible for particle internalization and intracellular trafficking.[3] This has included a range of studies across many different areas, including the potential of drug-free NPs for disease diagnosis and treatment,[4] the natural activities of NPs to combat multidrug-resistant pathogenic bacteria,[5] nanoprotein/nanocell interactions,[6] and their hemocompatibility[7,8] and immunoreactivity,[9] with studies often concentrating on their interaction with water molecules

Received: June 10, 2018
Accepted: August 22, 2018
Published: September 5, 2018

DOI: 10.1021/acsabm.8b00220
ACS Appl. Bio Mater. 2018, 1, 756−767

and subsequently how levels of hydration affect their behavior.[10]

Engineered nanoparticles are often designed to extend the circulation time of therapeutic drugs. However, despite the clear benefits of this strategy, their prolonged contact with blood components also has the potential to amplify adverse effects.[3] Injection of nanoparticles into the bloodstream can lead to activation of enzymes of the coagulation cascade, as well as platelets.[11] The complement system can also be activated, leading to opsonization and clearance of nanoparticles via the mononuclear phagocyte system (MPS).[12] Although there is no evidence that synthetic nanoparticles alone induce antigen-specific T cell responses, interactions with the innate immune system may indirectly impact adaptive immune responses through the production of inflammatory cytokines/chemokines and promotion of dendritic cell maturation.[13]

Within minutes of entering the bloodstream, nanoparticles are coated by plasma proteins (the protein "corona"), which play a critical role in determining the ensuing molecular and cellular responses to nanomaterials.[14] The composition of this protein corona is highly complex and variable but commonly includes albumin, immunoglobulins, complement proteins (including C3) and coagulation proteins (such as fibrinogen and coagulation factor (F) XII).[15,16] It is determined by the physicochemical characteristics of the material, including nanoparticle size[17] and surface charge.[18] For example, proteins with low isoelectric points (<5.5) preferably bind to positively charged particles whereas those with higher pI (>5.5) bind to negatively charged particles.[19]

The physicochemical characteristics of nanoparticles not only influence the selection of plasma proteins within the corona but also the type of interaction. The strength of protein binding, as well as conformational change[20] and denaturation,[21] is altered by hydrophobicity and surface charge. Such interactions can influence the coagulation response. For example, amine-modified nanoparticles reduce thrombin generation by depleting coagulation factors from the plasma, whereas binding to carboxy-modified, negatively charged nanoparticles initiates autoactivation of FXII by imposing specific orientation and order on the adsorbed protein molecules.[22] Nanoparticle size also has considerable influence, especially for sizes below 20−30 nm, as the high surface curvature impedes the formation of stable protein complexes due to steric hindrance as was shown for the association of coagulation cascade enzyme complexes.[18,23]

Immune reactivity and in vivo distribution of nanoparticles are also determined by size,[24,25] with small (10−20 nm) nanoparticles eliciting stronger pro-inflammatory cytokine responses, but larger particles (70−100 nm) delaying neutrophil apoptosis.[26] Small nanoparticles (3−8 nm) are rapidly cleared via the kidneys while larger particles are opsonized for recognition by phagocytic cells (neutrophils, monocytes, macrophages) and sequestration to liver and spleen.[27] Nanoparticle opsonization and clearance is additionally influenced by charge, with glomerular filtration being highest for small cationic particles, followed by neutral particles.[28] Opsonization is lower for neutral particles and can be minimized by the addition of moieties such as polyethylene glycol (PEG) to block electrostatic and hydrophobic interactions.[29] Negative surface charge is also an important factor in complement-mediated hypersensitivity reactions to liposome encapsulated drugs.[30] However, although complement activation is dependent on surface chemistry,[31,32] there is convincing evidence that complement component C3 binds to other plasma proteins within the corona, rather than directly to the nanoparticle surface.[15]

Our laboratory is developing small HBP nanoparticles as next-generation imaging agents for magnetic resonance imaging (MRI), positron emission tomography (PET) and optical imaging and also as therapeutics. Their hyperbranched structure facilitates the incorporation of multiple functionalities into a single molecule, thus making them ideal platforms for targeted drug delivery and diagnostic imaging.[24,33−35] Although these materials are well-characterized in terms of physicochemical properties (including morphology, particle size, surface charge, solubility), little attention has been directed to their hemocompatibility and immunoreactivity. Thus, this study used hyperbranched polymers (HBPs; ∼10 nm in diameter) to investigate how surface charge influences the swelling in water[10] and subsequent interaction of HBPs with components of whole human blood[36] as well as in vivo fate following i.v. injection into immunocompetent mice.

EXPERIMENTAL SECTION

HBP Synthesis. Hyperbranched polymers consisting of major components poly(ethylene glycol monomethyl ether methacrylate) (poly(PEGMA)), poly(2-(dimethylamino)ethyl methacrylate) (poly(DMAEMA)) or poly(methacrylic acid) ((poly(MAA)) were synthesized via the RAFT process using (((ethylthio)carbonothioyl)-thio)pentanoate (PCEPA) as RAFT agent as previously described (Supporting Information).[37] To monitor the fate of these nanoparticles in vivo, we incorporated Cy5 methacrylate monomer into each polymer as previously described.[38] To obtain endotoxin-free HBPs for injection, we sterilized all glassware used in synthesis by baking at 180 °C for 3 h) and all reagents were freshly prepared.

All pipet tips, plates, and water used in this study were certified endotoxin free, and procedures performed under sterile conditions in a class II biosafety cabinet unless otherwise stated. The chemical and physical properties of all polymers are presented in Table S1.

Endotoxin Assay. HBPs were dissolved in endotoxin-free water at a concentration of 100 μg mL^{-1}, and endotoxin levels determined by limulus amebocyte lysate (LAL) assay (Endosafe Portable Test System; Charles River, Wilmington, MA), according to the manufacturer's instructions.

Animal Experiments. Animal experiments were approved by the University of Queensland Animal Ethics Committee (AIBN/215/12/NHMRC/ARC) and complied with the Australian Code for the Care and Use of Animals for Scientific Purpose. CD1 mice (male, 6−8 weeks old) were provided by University of Queensland Biological Resources, and housed in the animal facility of the Centre for Advanced Imaging, with free access to water and food.

Hemocompatibility Assay. The hemocompatibility of neutral and charged hyperbranched polymeric nanoparticles was investigated by incubation with fresh whole human blood in a modified chandler loop. Fresh human blood was taken from healthy donors who had not taken any medication over the previous 10 days. Blood was drawn from the cubital vein with a 19G cannula and immediately anticoagulated with hirudin (Refludan, Celgene Munich, Germany; 1 μM). C-reactive protein (CRP) values were determined before performing subsequent tests, and samples excluded if they showed infectious or acute inflammatory symptoms (CRP > 10 μg mL^{-1}). For each study, blood from two ABO-compatible healthy volunteers was pooled and incubation commenced within 15 min of blood collection. Experiments were performed 4 times with n = 3 repeats each (except for elastase which was only detected for one experiment, n = 3). Reference values were obtained using silica nanospheres (Nano-Composix, Prague, Czech Republic) in 2 different sizes: 20 and 120 nm (n = 3). Silica nanospheres were delivered dispersed in water and used in a final concentration in blood of 200 μg mL^{-1}.

DOI: 10.1021/acsabm.8b00220
ACS Appl. Bio Mater. 2018, 1, 756−767

Chandler loop Tygon silicone tubes (type 3350, internal diameter 3.2 mm, length 55 cm) were cleaned sequentially with ethanol and water in an ultrasound bath, then closed to form a loop using a 4.8 mm internal diameter tube as a sheath and mounted on a vertical rotating disc. Stock solutions of HBP or silica nanospheres were mixed with hirudinized blood to a final sample concentration of 200 μg mL^{-1}. Tubes were filled to approximately 70% capacity with 3 mL blood containing nanoparticles, incubated and rotated (at 13 rpm) for 2 h at 37 °C and 5% CO_2. Following incubation, samples were prepared for analysis. Blood samples for cell counting and flow cytometry were analyzed immediately after incubation.

For detection of pro-thrombin fragment 1 + 2 (F1 + 2), platelet factor 4 (PF4), complement fragment C5a and PMN elastase, samples were mixed with the appropriate stabilizers (CTAD or EDTA), then frozen at −70 °C until analysis by ELISA for F1 + 2, (Enzygnost F1 + 2; Siemens Healthcare, Marburg, Germany), PF-4 (Hemochrom Diagnostica GmbH, Essen, Germany), C5a (DRG Instruments GmbH, Marburg, Germany) or elastase (BioVendor, Brno, Czech Republic) according to the manufacturers' instructions. Blood cell and platelet counts were performed on EDTA anticoagulated blood (Microvette, Sarstedt, Nümbrecht, Germany) using an automated cell counter (Coulter AcTdiff., Krefeld, Germany). Leukocyte activation (CD11b expression) and leukocyte-platelet conjugate formation were determined by flow cytometry (FacsCalibur, BD Biosciences, Heidelberg, Germany). Granulocytes were stained with VioBlue-labeled anti-CD11b (Miltenyi Biotec GmbH, Bergisch Gladbach, Germany). Platelet-granulocyte conjugates were detected by additional staining with FITC-labeled anti-CD41a (BD Biosciences) to identify platelets. Platelet activation was detected using a PE-labeled antihuman CD62p antibody (BD Biosciences). The attachment of Cy5-labeled nanoparticles to cells was also determined by flow cytometry and data analyzed using FlowJo software (Tree Star, Ashland, OR). Hemolysis was determined by detecting hemoglobin as cyanmethemoglobin photometrically at 540 nm after mixing diluted blood with Drabkin's reagent. For each experiment an individual calibration curve was performed. Results are given in relation to the initial sample to account for different initial values for each experiment.

Dendritic Cell Activation Assay. DC and T cell subsets within fresh human blood were studied for activation markers after incubation with HBPs using a modification of a previously described assay.[39] Blood was drawn from healthy human donors into sodium heparin vacuettes (Greiner Bio-One, Frickenhausen, Germany) after obtaining informed consent in accordance with University of Melbourne approved protocols.

Peripheral blood mononuclear cells (PBMC) were purified by density gradient centrifugation using Ficoll-Paque PLUS (GE Healthcare, Chicago, IL), and collected in RPMI 1640 (Life Technologies, Carlsbad, CA) + 10% fetal calf serum (Life Technologies) PBMC were transferred (1×10^6 cells well^{-1}) to U-bottomed 96-well plates and HBPs added to cells at final concentrations of 1, 10, or 100 μg mL-1. The TLR4 agonist lipopolysaccharide (LPS, 1 μg mL^{-1}) and TLR9 agonist CpG ODN 2216 (4.5 μM, InvivoGen; San Diego, CA) were used as positive controls. Cells were incubated for 6 h, 37°C in 5% CO2 incubator. Brefeldin A (BFA; Sigma) added after 4 h, then transferred to 5 mL polystyrene round-bottom tubes and washed with PBS. Cells were phenotyped by incubation with fluorochrome-conjugated monoclonal antibodies (mAb) against CD3 (total T lymphocytes), CD11c (DC and NK cells), CD14 (monocytes), CD16 (Fc receptor expressed by NK cells, activated monocytes, macrophages), CD19 (B cells), CD45 (total leukocytes) and CD123 (myeloid precursors, some B cells) at room temperature (RT) for 30 min. After washing, cells were fixed, then permeabilized using FACS Permeabilizing Solution 2 (BD Biosciences) and intracellular cytokines stained with mAbs against IL-8 and IFNα at RT for 1 h. Cells were washed and fixed with BD Stabilizing Fixative before FACS analysis. All mAbs were purchased from BD, except IL-8 (eBioscience) and CD123 (BioLegend). DCs were identified after applying their respective gating trees (Figure S5).

T Cell Activation Assay. Fresh heparinized whole blood (200 μL) was transferred directly into FACS tubes and HBPs added at final concentrations of 1, 10, or 100 μg mL^{-1}. Phorbol myristate acetate (PMA, 10 ng mL^{-1}) plus ionomycin (1 μg mL^{-1}) was used as a positive control. Blood was incubated for 6 h at 37°C in 5% CO_2 incubator. After 4 h, BFA added at 1x concentration and incubated for a further 2 h. Cells were washed and phenotyped with mAb against CD3, CD4, and CD8, then after further washing, cells fixed and permeabilized using BD FACS Permeabilizing Solution 2 and stained for intracellular cytokines by incubation with mAbs against CD154 (CD40L), TNF, and IFNγ at RT for 1 h. Cells were washed and fixed with BD Stabilizing Fixative. All mAbs were purchased from BD, except CD154 (Miltenyi Biotec).

Flow Cytometric Analysis. Stained and fixed cells were analyzed by flow cytometry (BD LSRFortessa) and data analyzed using FlowJo (v10). DCs or T cells were identified after applying their respective gating trees (see Figure S6).

Biodistribution Studies. Neutral, positively or negatively charged Cy5-HBPs (5 mg mL^{-1}, 150 μL; polymer solution) were freshly dissolved in PBS before i.v. injection via the retinal vein plexus into CD1 mice (n = 3/group) in a single dose. All mice were observed throughout the study period, and showed no clinical signs of ill health (altered gait, chills, lethargy or gross manifestation of stress) after HBP administration.

For imaging studies, CD1 mice were anesthetized with 2% isoflurane at predetermined intervals postinjection (1, 2, 6, 8, 12, and 24), and fluorescence and X-ray images obtained using an In Vivo MS FX Pro imaging station (Bruker, Germany). Cy5 fluorescence images were collected using a 630 nm excitation and 700 nm emission filter set (f-stop 2.80, 4 × 4 pixels binning, 180.00 mm FOV, 30 s exposure time), then overlaid with X-ray images (f-stop 2.51, 0.2 mm aluminum filter, 180 mm FOV, 30 s acquisition time) to provide anatomical information. All images were exported as 16 bit TIFF files and processed using Image-J (National Institute of Health). Upon termination, tissues of interest (heart, liver, spleen, lungs, kidney, and lymph node) were excised from all mice for ex vivo imaging.

Statistical Analyses. Results were analyzed using a non-parametric one-way ANOVA (Friedman test) followed by Dunn's multiple comparisons test or Tukeys multiple comparison test (GraphPad Prism 6). Results are presented as mean ± standard error.

RESULTS AND DISCUSSION

This research investigated cellular and molecular responses to small, hyperbranched polymeric nanoparticles of different charge, both ex vivo using whole human blood and in vivo following i.v. injection into mice. HBPs can be readily synthesized using robust methodologies, leading to materials with reproducible and tunable properties in terms of morphology, physical size, surface charge, etc.[40,41] They are thus regarded as an ideal matrix for drug or gene delivery vehicles as they are assumed to possess excellent biocompatibility, and the potential for biodegradability if required. Numerous reports have proved their applications in cancer therapy[42,43] or as imaging probes.[44] However, most of these studies focus on the synthesis of new chemical entities for particular bioapplications. To the best of our knowledge, there have been no systematic studies investigating their biocompatibility and immunoactivity ex vivo and in vivo.

To determine the effect of surface charge on hemocompatibility and immunoreactivity, three charge-varied HBPs were synthesized as previously reported;[41] Molecular weights were determined via a gel permeation chromatography (GPC) system equipped with multiangle laser light scattering (MALLS), while the molecular weight of each polymer arm was calculated via ^{1}H nuclear magnetic resonance (NMR). The hydrodynamic diameters and surface charges of HBPs were determined using dynamic light scattering (DLS). As

DOI: 10.1021/acsabm.8b00220
ACS Appl. Bio Mater. 2018, 1, 756−767

Scheme 1. Ex Vivo and in Vivo Analyses of Cellular and Molecular Responses to Charge-Varied HBPs

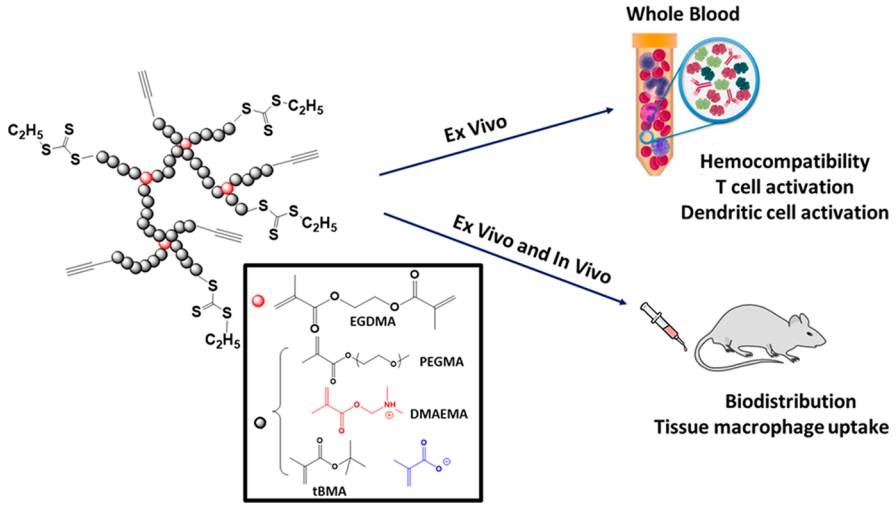

shown in Table S1, the three particles were similar in size (5 nm) and degree of branching (3−4). Most importantly, the zeta potential profiles of the three hyperbranched polymers were charged neutral (3.5 ± 0.2 mV), positive (+37.6 ± 0.4 mV) and negative (−33.1 ± 0.3) in water, respectively.

So that their fate could be monitored in vivo, HBPs were labeled with a fluorophore (Cy5) by incorporating Cy5 methacrylamide monomer; this near-infrared dye possesses low photon absorption and autofluorescence in living tissue and has previously been utilized for monitoring polymer behavior in mouse models.[45,33] The NMR of Cy5-HBPs and their UV−vis profiles are presented in Figure S1−S5. The overall approach for this research is depicted in Scheme 1.

Endotoxin Assay. Because endotoxin contamination may mask the true biological effects of nanoparticles,[46] we first established that HBP preparations were free of endotoxin before undertaking the analyses described in this report. Evaluation of endotoxin levels (Table 1) showed that all three

Table 1. Endotoxin Levels of Charge-Varied HBPs[a]

	spike recovery (%)	spike run time CV (%)	sample run time CV (%)	endotoxin level (EU mL^{-1})
standard	50−200	<25	<25	0.005−0.5
neutral HBP	104	6.4	6.3	<0.006
cationic HBP	56	1.6	1.3	<0.005
anionic HBP	89	3.3	3.2	<0.005

[a]Tests were considered valid if the CVs of replicate samples were <25% and spike recovery was between 50 and 200%. Values for all three HBP preparations were in this range.

HBPs had levels below 0.006 EU mL^{-1}, well below the recommended maximum values for intravenous administration of pharmaceutical products (less than 5 EU per kg body weight per hour),[47] and hence were suitable for the hemocompatibility and immunoreactivity investigations described in this paper.

Hemocompatibility Assays. The introduction of nanoparticles into the bloodstream may lead to serious and potentially life-threatening responses, including damage to erythrocytes (hemolysis), dysregulation of the coagulation system, thrombus formation and immune activation. The present study analyzed the molecular and cellular responses of whole human blood following exposure to charge-varied HBPs. Because silica is known to strongly activate the coagulation system, silica particles in 2 sizes (20 and 120 nm) served as positive control.[18,48]

Thrombin, the key enzyme of the blood coagulation cascade, can be activated when blood comes in contact with artificial materials.[49] In accord with previous studies showing that anionic surfaces are associated with increased coagulation,[50] incubation of human blood with anionic HBPs generated relatively higher levels of the prothrombin fragment 1 + 2 than neutral or cationic particles (F1 + 2; Figure 1A), but responses to all three HBPs were not significantly different from those generated by the negative control (blood incubated in a Chandler loop without particles). Overall, responses to HBPs were much lower than those generated following incubation with the negatively charged reference silica particles for which thrombin generation was 15- and 16.7-fold higher (for 20 and 120 nm sized beads, respectively) than the negative control. The very low values for HBPs are possibly due to their small size which may prevent the proper assembly of coagulation enzyme complexes.[23] Additionally, adsorption of coagulation enzymes by HBPs, and consequent depletion from the blood, may explain coagulation (F1 + 2) values lower than the control, as has been reported previously for amine-modified silica particles.[51]

In addition to activating soluble components of the coagulation system, injection of nanoparticles into the bloodstream may lead to platelet activation, and the consequent release of granule contents including platelet factor 4 (PF4), a promotor of coagulation.[52] As shown in Figure 1B, the platelet response was low for all three HBPs, with PF4 levels equal to, or lower than, the negative control value. The lowest PF4 values were obtained following incubation of whole blood with neutral particles, significantly lower than for anionic particles. Once again, silica particles induced significantly higher platelet degranulation, with levels 1.2- (silica 20 nm) and 1.4-fold (silica 120 nm) higher than the negative control. This result is in agreement with previous data showing that platelet activation is determined by hydrophobicity rather than charge.[53] Another indication of platelet activation showed the same trend with granulocyte-platelet

DOI: 10.1021/acsabm.8b00220
ACS Appl. Bio Mater. 2018, 1, 756−767

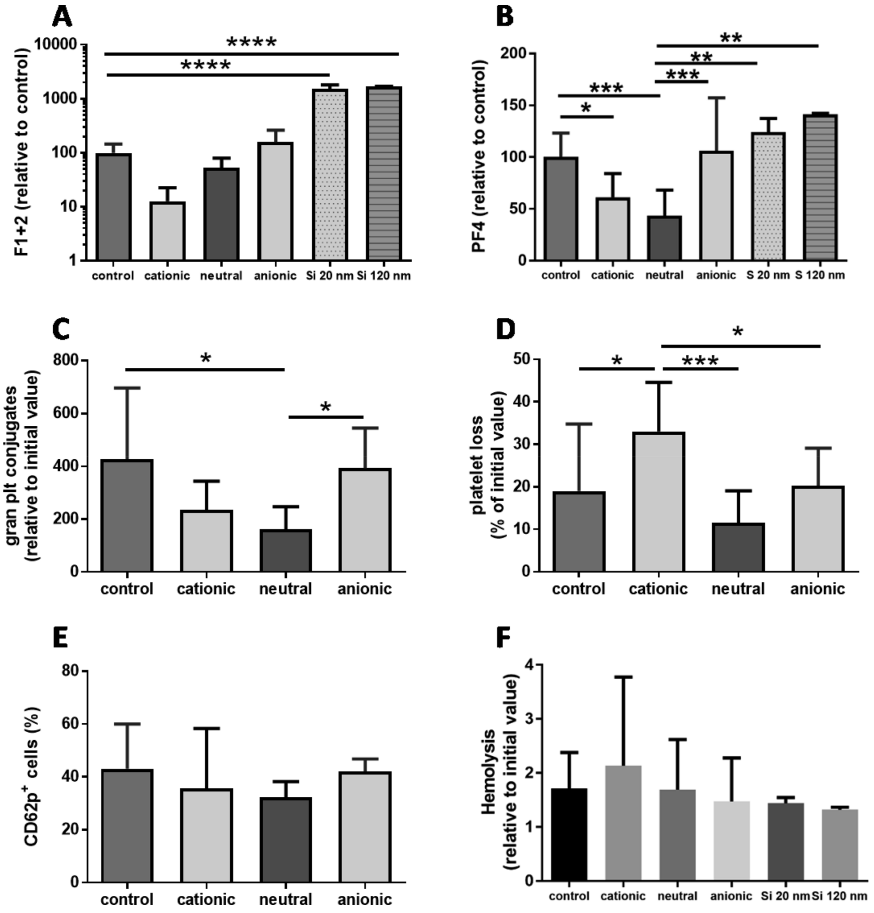

Figure 1. Effect of charge on HBP hemocompatibility. Anticoagulated whole blood was incubated alone (negative control) or with cationic, neutral, or anionic HBPs for 2 h in modified Chandler loops, then evaluated for (A) thrombin generation (F1 + 2), (B) platelet degranulation (PF4 release), (C) granulocyte-platelet conjugate formation, (D) platelet loss, (E) platelet activation (CD62p expression), and (F) hemolysis relative to the initial blood value (with 0.12% red blood cell lysis). Four experiments were performed independently with 3 replicates of each material summing up to $n = 12$ values per each hyperbranched material. Silica nanoparticles (20 and 120 nm) were added for one experiment as a positive reference (in total 3 values). $*p < 0.05$, $**p < 0.005$, $***p < 0.0005$, One-way ANOVA followed by Tukeys multicomparison test.

conjugate formation values for all three HBPs lower than or similar to the negative control (Figure 1C). Interestingly, conjugate formation in the presence of neutral particles was significantly lower than that for the negative control (blood incubated without HBPs). On the other hand, the reduction in platelet numbers was significantly greater following incubation of blood with cationic particles than for other HBPs (Figure 1D). Nevertheless platelet loss was much more distinct in response to silica particles, with platelet numbers 3.5- (20 nm) and 4.1-fold (120 nm) lower than the negative control. In agreement with previous suggestions that platelet-leukocyte conjugate formation is a more sensitive indicator of platelet activation than P selectin-positive cells,[54] incubation with HBP preparations failed to alter the percentage of CD62p-positive cells. Overall, these findings are consistent with previous studies showing minimal effects of branched macromolecules (e.g., hyperbranched polyglycerol[55]) on either enzymes of the coagulation cascade or platelet activation.

We have previously investigated the HBP in a static hemolysis assay using mouse red blood cells (RBCs).[41] While anionic and neutral HBPs did not cause hemolysis, cationic HBPs displayed a concentration dependent hemoglobin release following 3 h incubation at RT. In this report, we use a different experimental method to evaluate HBPs hemolysis profile with whole human blood, potentially providing a more robust method for testing the potential of HBPs to damage blood cells. As shown in Figure 1F, none of the HBPs caused significant hemolysis following rotated incubation (13 rpm) with whole blood at 37 °C for 2 h, indicated by a degree of lysis less than 1%. In all cases, pH changes in blood were minimal over the 2 h incubation period, with values remaining within the physiological range, and not significantly different from the control. Collectively, the hemocompatibility data confirm that HBPs have a wide safety margin for blood-contact applications and are thus suitable for intravenous administration.

Immune Reactivity. The potential for HBPs to be recognized by the innate immune system was investigated by incubating nanoparticles with whole human blood, then measuring complement activation (by detection of the complement activation product, C5a) and granulocyte activation (CD11b expression, elastase release and granulocyte loss) (Figure 2). Analysis of C5a levels following incubation of HBPs with human blood (Figure 2A) showed that complement activation in response to neutral HBPs was minimal, not significantly different from the negative control (blood incubated without nanoparticles) but significantly lower than for either anionic (4.23 ± 1.39 $\mu g\ l^{-1}$ C5a) or cationic (5.00 ± 0.85 $\mu g\ l^{-1}$ C5a) particles. The 20 nm silica spheres induced moderate complement activation (5.8 ± 0.4 $\mu g\ l^{-1}$ C5a),

DOI: 10.1021/acsabm.8b00220
ACS Appl. Bio Mater. 2018, 1, 756−767

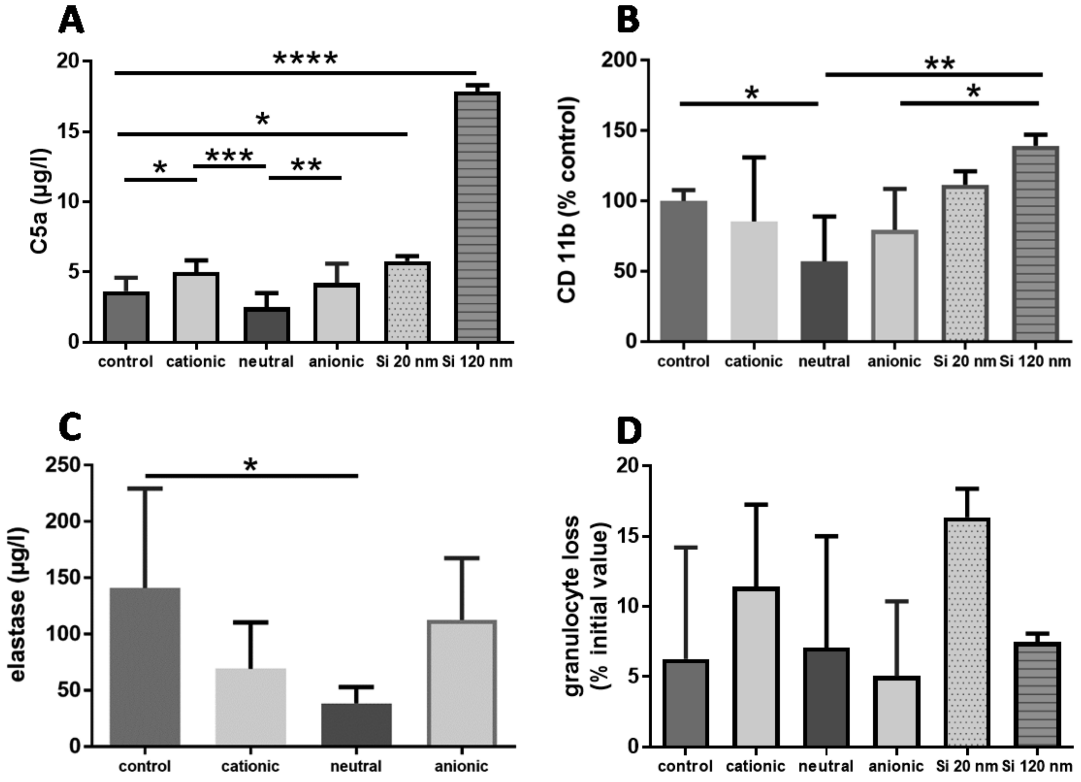

Figure 2. Effect of charge on innate immune responses to HBPs, evaluated by (A) complement activation (C5a), (B) granulocyte activation (CD11b), (C) elastase release, and (D) granulocyte loss following in vitro incubation of HBP with anticoagulated fresh, whole human blood for 2 h in modified Chandler loops. Data expressed as mean ± SD; *p < 0.05, **p < 0.005, ***p < 0.0005, one-way ANOVA, with Tukeys multicomparison test.

similar to charged HBPs, while larger (120 nm) silica spheres induced a much greater response (17.9 ± 0.4 μg l^{-1} C5a), suggesting that the assembly of complement complexes was limited on the smaller silica particles.

Granulocytes play a key role in innate immunity, and are the first cells recruited to the site of infection. Although normally short-lived (12−24 h in the circulation), neutrophil life-span can be prolonged following activation by foreign material, so that this material can be phagocytosed.[56] Conversely granulocyte activation can lead to degranulation and release of pro-inflammatory mediators such as reactive oxygen species (ROS) and elastase which promote the formation of neutrophil extracellular traps (NETs).[57] Granulocyte activation (indicated by cell surface CD11b expression and elastase release; Figures 2 b and c) in the presence of neutral HBPs was significantly lower than in the absence of nanoparticles (negative control). However, the reduction in granulocyte numbers was not significantly different between groups, indicating that HBPs had no significant effect on the rate of neutrophil apoptosis. It also suggests that HBPs do not induce NET formation, in contrast to small (15 nm) silver nanoparticles which have recently been shown to stimulate NET release by human neutrophils.[58] Although larger silica particles induced significant complement activation and increased CD11b expression compared to neutral and anionic particles, they had no significant effect on granulocyte numbers.

Following the incubation of HBPs with human blood cells (platelets, granulocytes and monocytes), neutral HBPs demonstrated the lowest attachment to these three cell types. For monocytes, cationic HBPs demonstrated slightly higher binding than anionic HBPs. This result is in agreement with our previous demonstration that cationic HBPs had the highest uptake by the RAW264.7 murine macrophage cell line,[41] and may reflect the interaction of cationic HBPs with scavenger receptors on the cell surface (as previously reported for a range of cationic polymers, lipids and polypeptides).[59] In contrast, granulocytes had the greatest association with anionic HBPs, which is in agreement with studies by us and others that suggest anionic nanoparticles are preferentially ingested by certain phagocytic cells.[37] The small size of the HBPs used in this study suggests that they are likely taken up by mechanisms other than conventional phagocytosis.[60]

Platelets associated greatest with cationic Cy5-HBPs, while association with anionic HBPs was approximately 50% less (Figure 3). These results can be examined in the context of Figure 1, which showed greater platelet loss in response to cationic nanoparticles, yet significant platelet activation

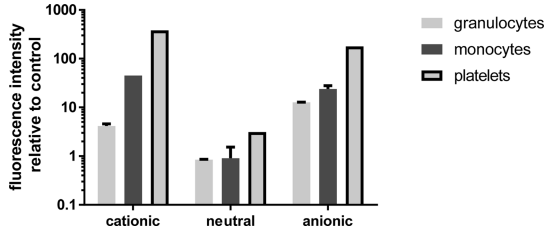

Figure 3. Effect of charge on interaction of HBPs with innate immune cells. Histogram shows the fluorescence intensities for charge-varied Cy5-labeled nanoparticles attached to granulocytes, monocytes or platelets determined in one single experiment.

DOI: 10.1021/acsabm.8b00220
ACS Appl. Bio Mater. 2018, 1, 756−767

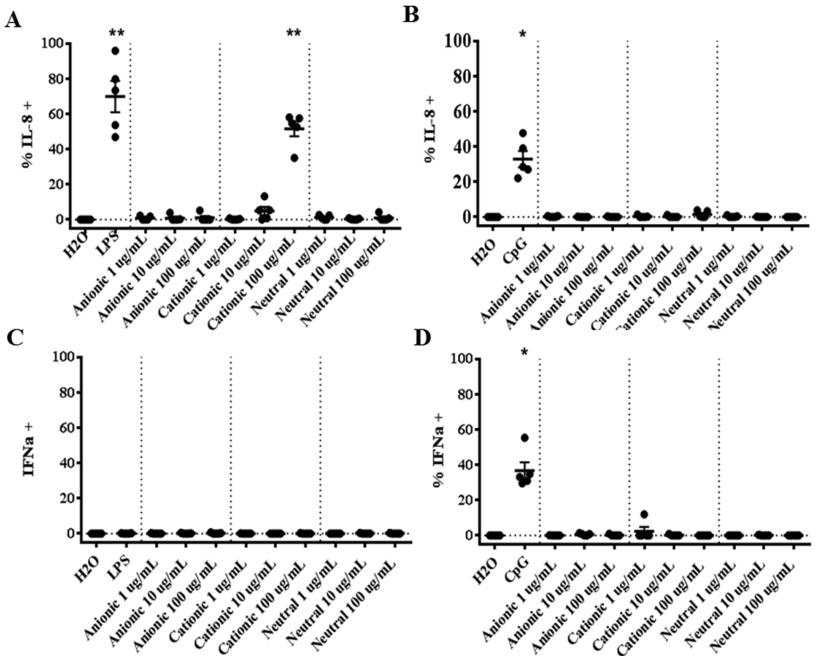

Figure 4. Human DC activation is dependent on HBP surface charge. HBPs were incubated with fresh PBMC from healthy human donors for 6 h at 37°C. The activation of (A, C) gated myeloid dendritic cells (mDC) and (B, D) plasmacytoid dendritic cells (pDC; see Figure S5 for gating strategy) was indicated by intracellular cytokine staining for (A, B) IL-8 or (C, D) IFNα. * $p < 0.05$, ** $p < 0.01$ (vs H2O). Friedman test with Dunn's multiple comparisons. DC, dendritic cell; IL-8, interleukin-8; IFNa, interferon α; HBP, hyperbranched polymer; LPS, lipopolysaccharide.

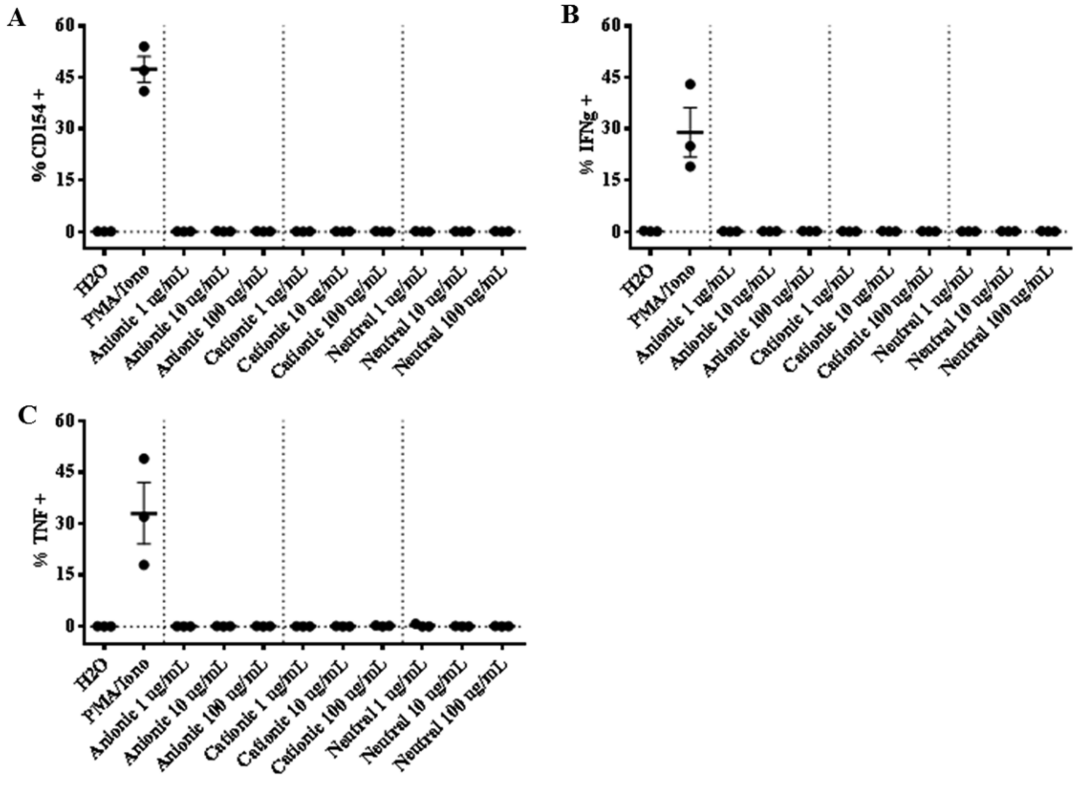

Figure 5. Primary human T cells are not activated by HBPs. HBPs were added to freshly drawn heparinized human blood and incubated for 6 h at 37°C, and the activation state of T cells was then determined by intracellular cytokine staining for (A) CD154, (B) IFNγ, or (C) TNF. Stimulation with PMA/Ionomycin served as a positive control for T cell activation.

(indicated by increased PF4 release) in response to anionic nanoparticles. Further studies are warranted to elucidate the biological mechanisms between HBP charge and platelet activation versus cell loss.

Dendritic Cell Activation Evaluation. Depending on their application, for example as vaccine adjuvants or drug delivery vehicles, nanoparticles can be designed to either stimulate or evade an immune response.[61] Dendritic cells

DOI: 10.1021/acsabm.8b00220
ACS Appl. Bio Mater. 2018, 1, 756−767

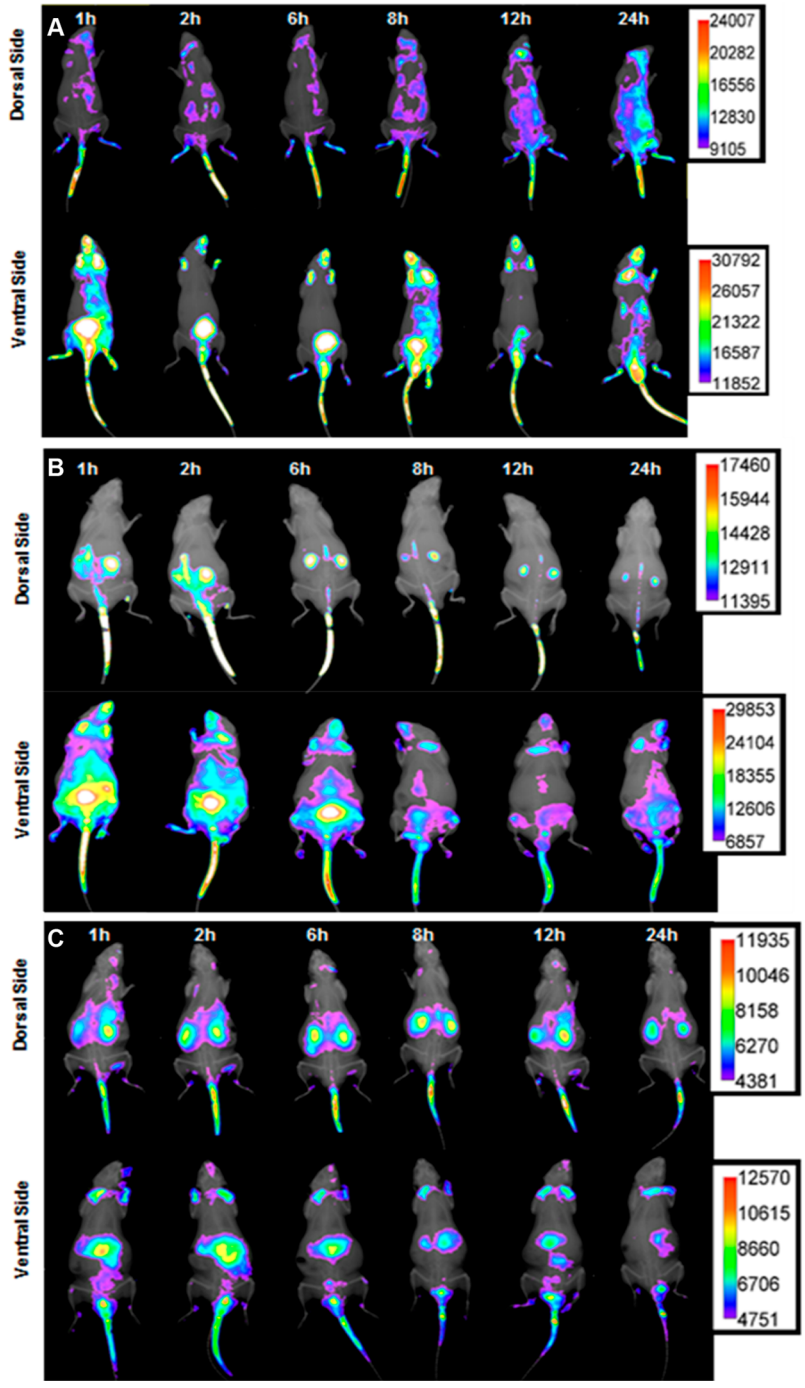

Figure 6. In vivo biodistribution of HBPs. Fluorescence images show representative CD1 mice (dorsal and ventral sides) at 1, 2, 6, 8, 12, and 24 h after i.v. injection of (A) neutral, (B) cationic, or (C) anionic Cy5-HBPs.

(DC) are the most efficient antigen presenting cells and play a critical role in the adaptive immune response to pathogens and vaccines. Effective priming of naïve lymphocytes will only occur if these agents activate DCs to release cytokine messengers, such as interleukin (IL)-8 or interferon (IFN)-α, depending on whether they are myeloid (conventional) CD11c+ DCs (mDC) or plasmacytoid CD123+ DCs (pDC).[62] DCs are capable of internalizing nanoengineered materials, such as latex particles and liposomes, and the induction of cytotoxic T lymphocyte (CTL) responses have been reported to be similar to those induced by protein antigens.[39] Examination of the effect of HBPs on CD11c+ mDC activation showed a charge-dependence (Figure 4 A, B), with cationic HBPs (at a concentration of 100 μg mL^{-1}) stimulating IL-8 expression (51.7 ± 4.3% IL-8+ cells), while neutral and anionic HBPs had little effect at this concentration (1.0 ± 0.8% and 1.0 ± 1.0% IL-8+ cells respectively). In contrast, neither cationic, anionic nor neutral HBPs activated pDCs as evidenced by their negligible secretion of type I IFN (IFN-α) (Figure 4 C, D). Taken together, these results suggest that neutral and anionic particles might be more useful for drug delivery applications, whereas cationic particles may hold utility for vaccine delivery where mDC activation is desired. Indeed, it is notable that cationic liposomes (e.g., 1,2-dioleoyl-

DOI: 10.1021/acsabm.8b00220
ACS Appl. Bio Mater. 2018, 1, 756−767

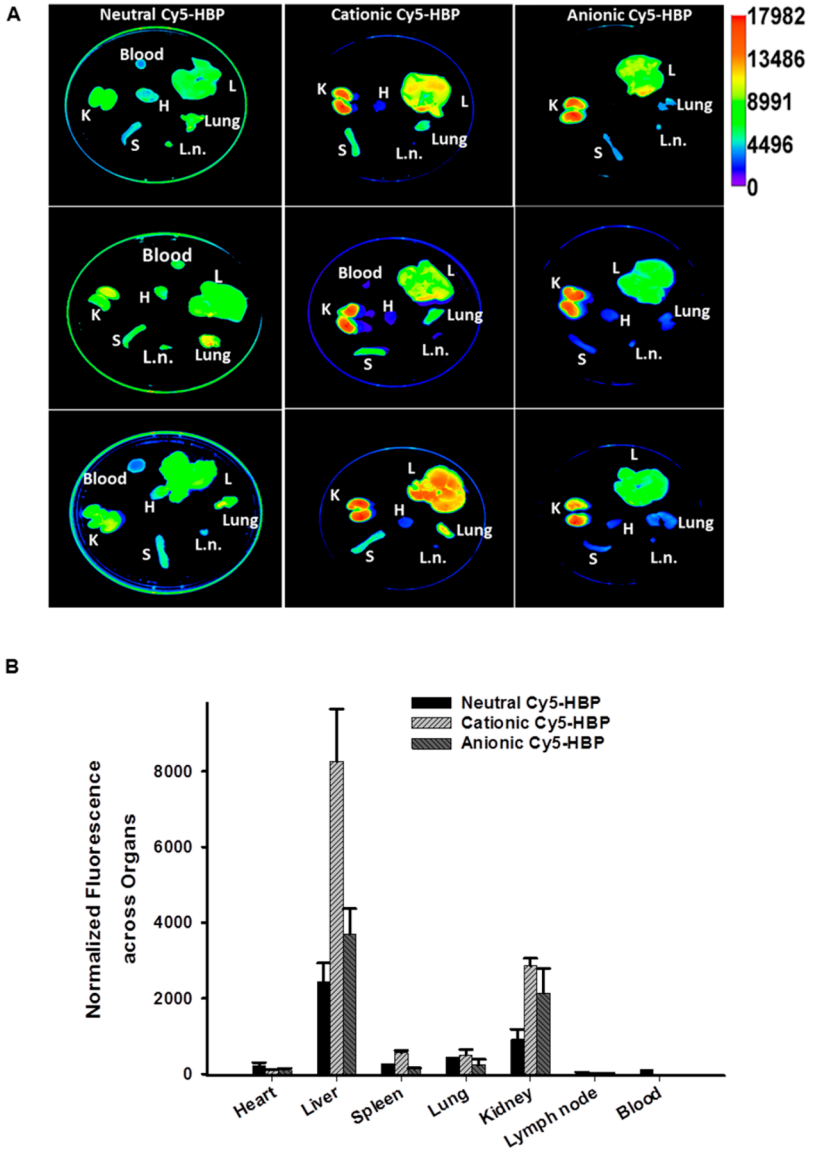

Figure 7. Biodistribution of HBPs. (A) Normalized fluorescence images of organs excised from CD1 mice 24 h post i.v. injection of charge-varied Cy5- HBPs (h = heart, l = liver, s = spleen, l.n.= lymph node). (B) Bar chart showing normalized fluorescence intensities of excised organs. For all samples, background signal was subtracted using ImageJ (mean ± SD; n = 3/group).

3-trimethylammoninum propane (DOTAP), and dimethyldioctadecylammonium (DDA)) have been demonstrated to promote DC maturation and are commonly used experimental adjuvants.[63,64]

T Cell Activation Assay. As effector cells of the adaptive immune system, CD3+ T lymphocytes respond to antigens specific for their T cell receptor. This leads to up-regulated expression of cell surface and intracellular activation markers, along with clonal expansion as either helper (CD4+) or cytotoxic (CD8+) T cells. Activated T cells can secrete IFN-γ and tumor necrosis factor (TNF),[65] and up-regulate expression of the natural ligand to the CD40 receptor (CD40L; CD154) on antigen presenting cells.[66] Incubation of cationic, anionic or neutral HBP with fresh human blood did not induce expression of these T cell activation markers (Figure 5), suggesting that their presence in blood does not cause significant levels of T cell activation under the conditions tested.

In Vivo Biodistribution of HBPs. Depending on their size and functionality, hyperbranched polymers have been reported to remain in the circulation of mice for over 24 h.[67] Having demonstrated that the three polymers showed limited or no activation of either innate or adaptive immunity, we next attempted to correlate ex vivo analyses with in vivo behavior of these materials by monitoring the biodistribution of each HBP over a 24 h time-course following i.v. injection into healthy, immunocompetent CD1 mice (Figure 6). Although the mononuclear phagocyte system (MPS) organs (e.g., liver and spleen) are typical accumulation sites for i.v. delivered nanoparticles, hydrophilic polyethylene glycol (PEG) has been reported to have reduced MPS uptake.[29] In this study, neutral HBPs tended to remain in the circulation without retention by MPS organs, and were mainly cleared via the bladder, likely as a result of simple filtration by renal glomeruli. This suggests that PEG-based particles maintain their molecular integrity, are minimally altered by possible protein adsorption in the bloodstream and, in accord with previous

DOI: 10.1021/acsabm.8b00220
ACS Appl. Bio Mater. 2018, 1, 756−767

reports, are shielded from immune recognition.[29] It is consistent with our ex vivo analyses that showed neutral HBPs were relatively inert to immune recognition (indicated by their lack of complement, DC or T cell activation). It is also in accord with our previous demonstration that neutral HBPs have the longest half-life in serum, approximately 6 h.[41] In contrast to neutral HBPs (Figure 6A), charged HBPs displayed a rapid accumulation in clearance organs (liver and kidney) postadministration (Figure 6B, C; 1 h postinjection).

Results were confirmed by *ex vivo* fluorescence imaging of organs excised 24 h postinjection which showed that fluorescence signals from neutral HBPs were still detectable in the blood, whereas fluorescence from cationic HBPs had almost disappeared (Figure 7A, B). Neutral HBPs also showed relatively high fluorescence in the heart, likely reflecting their longer circulation half-life and higher blood concentrations. In contrast, cationic and anionic samples showed highest retention in the liver (Figure 7), suggesting increased uptake of these particles by the MPS. Furthermore, spleen fluorescence was relatively stronger following administration of cationic HBPs, leading us to hypothesize that cationic HBPs may be phagocytized by resident macrophages within the liver (Kupffer cells) and spleen.[68] Phagocytes have previously demonstrated a preference for internalizing anionic nanoparticles,[69] however the small size of the HBPs used in the present study suggest that other uptake mechanisms may be involved. Previously reported studies suggest that serum protein adsorption (as would occur in the circulation) not only increases nanoparticle size but also imparts a net negative charge on both anionic and cationic nanoparticles.[59] The formation of these protein complexes with cationic nanoparticles promotes cell binding via scavenger receptors, pattern recognition receptors which are expressed on a range of cell types including macrophages, dendritic cells, endothelial cells, and epithelial cells, and are capable of recognizing negatively charged foreign particles.[70]

CONCLUSION

Understanding how the physicochemical properties of HBPs determine their effect on blood coagulation, the immune system, and biodistribution, is essential to the development of these nanomaterials for various biomedical applications. This paper demonstrates that the surface charge of HBPs influences their in vivo behavior in terms of circulation time, tissue distribution, and clearance from the body, and suggests a mechanism by which nanoparticles can be tailored for particular biomedical applications.

Ex vivo evaluation of charge-varied HBPs using whole human blood demonstrated their hemocompatibility. These polymers did not induce platelet activation, coagulation, hemolysis or complement activation. Although there was no evidence of a T cell response to any of the HBPs, high concentrations of the cationic particles (but not neutral or anionic particles) led to myeloid DC activation, indicating their potential application as vaccine adjuvants to aid efficient antigen presentation. Biodistribution studies showed that PEG-based charge-neutral HBPs had a longer retention time in the circulation and were eventually cleared in the urine, whereas charged HBPs mainly accumulated in liver and spleen and were cleared more rapidly from the circulation. It is worth noting that vaccines are usually administered via subcutaneous injection, intramuscular administration or intradermal routes. Therefore, the biodistribution study described in this paper will be applicable to HBP vaccine indication only if the particles distribute systemically. A thorough investigation of the mode-of-administration and distribution from the site of injection of such vaccine will be evaluated separately as it was outside the scope of the present study. Our results demonstrate the importance of nanoparticle surface charge in determining their in vivo fate, and suggest that the manipulation of surface charge may be an important mechanism to tailor particles for different applications. These studies help to develop a fundamental understanding of HBP behavior in the blood, and how their physicochemical properties influence cellular uptake and distribution in vivo. They may also aid in the establishment of guidelines and protocols that assist in the development of efficient and safe drug delivery platforms.

ASSOCIATED CONTENT

Supporting Information

The Supporting Information is available free of charge on the ACS Publications website at DOI: 10.1021/acsabm.8b00220.

Details of polymer synthesis, polymer properties, NMR spectra, UV−vis spectra, and flow cytometry gating strategies for ex vivo whole blood assays (PDF)

AUTHOR INFORMATION

Corresponding Authors

*E-mail: k.thurecht@uq.edu.au.
*E-mail: b.rolfe@uq.edu.au.

ORCID

Robert De Rose: 0000-0003-4316-3910
Claudia Sperling: 0000-0002-8509-9382
Stephen J. Kent: 0000-0002-8539-4891
Zachary H. Houston: 0000-0001-9738-4917
Kristofer J. Thurecht: 0000-0002-4100-3131

Author Contributions

The hemocompatibility assays were conducted by L.C., C.S.; T-cell/dendritic cell assays by J.G.; in vivo imaging by L.C., N.F., Z.H.; B.R., K.J.T., C.S., R.R., and S.K. contributed to intellectual input and framing of the manuscript concepts. The manuscript was written through contributions of all authors. All authors have given approval to the final version of the manuscript.

Notes

The authors declare no competing financial interest.

ACKNOWLEDGMENTS

The authors acknowledge the Australian Research Council (LP150100703 (K.J.T.), DP140100951 (K.J.T.)) and National Health and Medical Research Council (APP1099321, APP1148582 (K.J.T.), APP1148582 (B.E.R.)) for funding. This work was performed in part at the Queensland node of the Australian National Fabrication Facility (ANFF), a company established under the National Collaborative Research Infrastructure Strategy to provide nano- and microfabrication facilities for Australia's researchers. This research was conducted and funded in part by the ARC Centre of Excellence in Convergent Bio-Nano Science and Technology (CE140100036), the National Imaging Facility (NIF), and a grant from the University of Queensland Collaboration and Industry Engagement Fund. L.C. thanks the Chinese Scholarship Council for financial support.

DOI: 10.1021/acsabm.8b00220
ACS Appl. Bio Mater. 2018, 1, 756−767

ABBREVIATIONS

HBP, hyperbranched polymer; NPs, nanoparticles; i.v., intravenous injection; CRP, C-reactive protein; FACS, fluorescence-activated cell sorting.

REFERENCES

(1) Gupta, A. S. Nanomedicine Approaches in Vascular Disease: A Review. *Nanomedicine* **2011**, *7* (6), 763−779.

(2) Bobo, D.; Robinson, K. J.; Islam, J.; Thurecht, K. J.; Corrie, S. R. Nanoparticle-Based Medicines: A Review of Fda-Approved Materials and Clinical Trials to Date. *Pharm. Res.* **2016**, *33* (10), 2373−2387.

(3) Dobrovolskaia, M. A.; McNeil, S. E. Immunological Properties of Engineered Nanomaterials: An Introduction. *Front. Nanobiomed. Res.* **2013**, *1*, 1−23.

(4) Thurecht, K. J.; Blakey, I.; Peng, H.; Squires, O.; Hsu, S.; Alexander, C.; Whittaker, A. K. Functional Hyperbranched Polymers: Toward Targeted in Vivo 19f Magnetic Resonance Imaging Using Designed Macromolecules. *J. Am. Chem. Soc.* **2010**, *132* (15), 5336−5337.

(5) Li, X. N.; Robinson, S. M.; Gupta, A.; Saha, K.; Jiang, Z. W.; Moyano, D. F.; Sahar, A.; Riley, M. A.; Rotello, V. M. Functional Gold Nanoparticles as Potent Antimicrobial Agents against Multi-Drug-Resistant Bacteria. *ACS Nano* **2014**, *8* (10), 10682−10686.

(6) Nel, A. E.; Madler, L.; Velegol, D.; Xia, T.; Hoek, E. M. V.; Somasundaran, P.; Klaessig, F.; Castranova, V.; Thompson, M. Understanding Biophysicochemical Interactions at the Nano-Bio Interface. *Nat. Mater.* **2009**, *8* (7), 543−557.

(7) Venault, A.; Hsu, K.-J.; Yeh, L.-C.; Chinnathambi, A.; Ho, H.-T.; Chang, Y. Surface Charge-Bias Impact of Amine-Contained Pseudozwitterionic Biointerfaces on the Human Blood Compatibility. *Colloids Surf., B* **2017**, *151*, 372−383.

(8) Shih, Y.-J.; Chang, Y.; Quemener, D.; Yang, H.-S.; Jhong, J.-F.; Ho, F.-M.; Higuchi, A.; Chang, Y. Hemocompatibility of Polyampholyte Copolymers with Well-Defined Charge Bias in Human Blood. *Langmuir* **2014**, *30* (22), 6489−6496.

(9) Min, Y. Z.; Roche, K. C.; Tian, S. M.; Eblan, M. J.; McKinnon, K. P.; Caster, J. M.; Chai, S. J.; Herring, L. E.; Zhang, L. Z.; Zhang, T.; DeSimone, J. M.; Tepper, J. E.; Vincent, B. G.; Serody, J. S.; Wang, A. Z. Antigen-Capturing Nanoparticles Improve the Abscopal Effect and Cancer Immunotherapy. *Nat. Nanotechnol.* **2017**, *12* (9), 877−882.

(10) Zheng, J.; Li, L.; Chen, S.; Jiang, S. Molecular Simulation Study of Water Interactions with Oligo (Ethylene Glycol)-Terminated Alkanethiol Self-Assembled Monolayers. *Langmuir* **2004**, *20* (20), 8931−8938.

(11) Frohlich, E. Action of Nanoparticles on Platelet Activation and Plasmatic Coagulation. *Curr. Med. Chem.* **2016**, *23* (5), 408−430.

(12) Owens, D. E., III; Peppas, N. A. Opsonization, Biodistribution, and Pharmacokinetics of Polymeric Nanoparticles. *Int. J. Pharm.* **2006**, *307* (1), 93−102.

(13) Yang, E. J.; Kim, S.; Kim, J. S.; Choi, I. H. Inflammasome Formation and Il-1beta Release by Human Blood Monocytes in Response to Silver Nanoparticles. *Biomaterials* **2012**, *33* (28), 6858−6867.

(14) Fleischer, C. C.; Payne, C. K. Nanoparticle−Cell Interactions: Molecular Structure of the Protein Corona and Cellular Outcomes. *Acc. Chem. Res.* **2014**, *47* (8), 2651−2659.

(15) Chen, F.; Wang, G.; Griffin, J. I.; Brenneman, B.; Banda, N. K.; Holers, V. M.; Backos, D. S.; Wu, L.; Moghimi, S. M.; Simberg, D. Complement Proteins Bind to Nanoparticle Protein Corona and Undergo Dynamic Exchange in Vivo. *Nat. Nanotechnol.* **2017**, *12* (4), 387−393.

(16) Dobrovolskaia, M. A.; Neun, B. W.; Man, S.; Ye, X.; Hansen, M.; Patri, A. K.; Crist, R. M.; McNeil, S. E. Protein Corona Composition Does Not Accurately Predict Hematocompatibility of Colloidal Gold Nanoparticles. *Nanomedicine* **2014**, *10* (7), 1453−1463.

(17) Lundqvist, M.; Stigler, J.; Elia, G.; Lynch, I.; Cedervall, T.; Dawson, K. A. Nanoparticle Size and Surface Properties Determine the Protein Corona with Possible Implications for Biological Impacts. *Proc. Natl. Acad. Sci. U. S. A.* **2008**, *105* (38), 14265−14270.

(18) Kushida, T.; Saha, K.; Subramani, C.; Nandwana, V.; Rotello, V. M. Effect of Nano-Scale Curvature on the Intrinsic Blood Coagulation System. *Nanoscale* **2014**, *6* (23), 14484−14487.

(19) Gessner, A.; Lieske, A.; Paulke, B. R.; Muller, R. H. Influence of Surface Charge Density on Protein Adsorption on Polymeric Nanoparticles: Analysis by Two-Dimensional Electrophoresis. *Eur. J. Pharm. Biopharm.* **2002**, *54* (2), 165−170.

(20) Lacerda, S. H.; Park, J. J.; Meuse, C.; Pristinski, D.; Becker, M. L.; Karim, A.; Douglas, J. F. Interaction of Gold Nanoparticles with Common Human Blood Proteins. *ACS Nano* **2010**, *4* (1), 365−379.

(21) Roach, P.; Farrar, D.; Perry, C. C. Interpretation of Protein Adsorption: Surface-Induced Conformational Changes. *J. Am. Chem. Soc.* **2005**, *127* (22), 8168−8173.

(22) Chen, X.; Wang, J.; Paszti, Z.; Wang, F.; Schrauben, J. N.; Tarabara, V. V.; Schmaier, A. H.; Chen, Z. Ordered Adsorption of Coagulation Factor Xii on Negatively Charged Polymer Surfaces Probed by Sum Frequency Generation Vibrational Spectroscopy. *Anal. Bioanal. Chem.* **2007**, *388* (1), 65−72.

(23) Sanfins, E.; Augustsson, C.; Dahlback, B.; Linse, S.; Cedervall, T. Size-Dependent Effects of Nanoparticles on Enzymes in the Blood Coagulation Cascade. *Nano Lett.* **2014**, *14* (8), 4736−4744.

(24) Rolfe, B. E.; Blakey, I.; Squires, O.; Peng, H.; Boase, N. R.; Alexander, C.; Parsons, P. G.; Boyle, G. M.; Whittaker, A. K.; Thurecht, K. J. Multimodal Polymer Nanoparticles with Combined 19f Magnetic Resonance and Optical Detection for Tunable, Targeted, Multimodal Imaging in Vivo. *J. Am. Chem. Soc.* **2014**, *136* (6), 2413−2419.

(25) Soo Choi, H.; Liu, W.; Misra, P.; Tanaka, E.; Zimmer, J. P.; Itty Ipe, B.; Bawendi, M. G.; Frangioni, J. V. Renal Clearance of Quantum Dots. *Nat. Biotechnol.* **2007**, *25* (10), 1165−1170.

(26) Poirier, M.; Simard, J. C.; Girard, D. Silver Nanoparticles of 70 Nm and 20 Nm Affect Differently the Biology of Human Neutrophils. *J. Immunotoxicol.* **2016**, *13* (3), 375−385.

(27) Longmire, M.; Choyke, P. L.; Kobayashi, H. Clearance Properties of Nano-Sized Particles and Molecules as Imaging Agents: Considerations and Caveats. *Nanomedicine* **2008**, *3* (5), 703−717.

(28) Deen, W. M.; Lazzara, M. J.; Myers, B. D. Structural Determinants of Glomerular Permeability. *Am. J. Physiol Renal Physiol* **2001**, *281* (4), F579−596.

(29) Amoozgar, Z.; Yeo, Y. Recent Advances in Stealth Coating of Nanoparticle Drug Delivery Systems. *Wiley Interdiscip Rev. Nanomed Nanobiotechnol* **2012**, *4* (2), 219−233.

(30) Szebeni, J.; Bedocs, P.; Rozsnyay, Z.; Weiszhar, Z.; Urbanics, R.; Rosivall, L.; Cohen, R.; Garbuzenko, O.; Bathori, G.; Toth, M.; Bunger, R.; Barenholz, Y. Liposome-Induced Complement Activation and Related Cardiopulmonary Distress in Pigs: Factors Promoting Reactogenicity of Doxil and Ambisome. *Nanomedicine* **2012**, *8* (2), 176−184.

(31) Sperling, C.; Maitz, M. F.; Talkenberger, S.; Gouzy, M. F.; Groth, T.; Werner, C. In Vitro Blood Reactivity to Hydroxylated and Non-Hydroxylated Polymer Surfaces. *Biomaterials* **2007**, *28* (25), 3617−3625.

(32) Sou, K.; Tsuchida, E. Electrostatic Interactions and Complement Activation on the Surface of Phospholipid Vesicle Containing Acidic Lipids: Effect of the Structure of Acidic Groups. *Biochim. Biophys. Acta, Biomembr.* **2008**, *1778* (4), 1035−1041.

(33) Pearce, A. K.; Rolfe, B. E.; Russell, P. J.; Tse, B. W. C.; Whittaker, A. K.; Fuchs, A. V.; Thurecht, K. J. Development of a Polymer Theranostic for Prostate Cancer. *Polym. Chem.* **2014**, *5* (24), 6932−6942.

(34) Tan, J. H.; McMillan, N. A. J.; Payne, E.; Alexander, C.; Heath, F.; Whittaker, A. K.; Thurecht, K. J. Hyperbranched Polymers as Delivery Vectors for Oligonucleotides. *J. Polym. Sci., Part A: Polym. Chem.* **2012**, *50* (13), 2585−2595.

(35) Ardana, A.; Whittaker, A. K.; Thurecht, K. J. Peg-Based Hyperbranched Polymer Theranostics: Optimizing Chemistries for Improved Bioconjugation. *Macromolecules* **2014**, *47* (15), 5211−5219.

DOI: 10.1021/acsabm.8b00220
ACS Appl. Bio Mater. 2018, 1, 756−767

(36) Hall, J. B.; Dobrovolskaia, M. A.; Patri, A. K.; McNeil, S. E. Characterization of Nanoparticles for Therapeutics. *Nanomedicine* **2007**, *2* (6), 789−803.
(37) Glass, J. J.; Chen, L.; Alcantara, S.; Crampin, E. J.; Thurecht, K. J.; De Rose, R.; Kent, S. J. Charge Has a Marked Influence on Hyperbranched Polymer Nanoparticle Association in Whole Human Blood. *ACS Macro Lett.* **2017**, *6*, 586−592.
(38) Ma, Y.; Fuchs, A. V.; Boase, N. R. B.; Rolfe, B. E.; Coombes, A. G. A.; Thurecht, K. J. The in Vivo Fate of Nanoparticles and Nanoparticle-Loaded Microcapsules after Oral Administration in Mice: Evaluation of Their Potential for Colon-Specific Delivery. *Eur. J. Pharm. Biopharm.* **2015**, *94*, 393−403.
(39) De Rose, R.; Zelikin, A. N.; Johnston, A. P.; Sexton, A.; Chong, S. F.; Cortez, C.; Mulholland, W.; Caruso, F.; Kent, S. J. Binding, Internalization, and Antigen Presentation of Vaccine-Loaded Nano-engineered Capsules in Blood. *Adv. Mater.* **2008**, *20* (24), 4698−4703.
(40) Liu, B. L.; Kazlauciunas, A.; Guthrie, J. T.; Perrier, S. One-Pot Hyperbranched Polymer Synthesis Mediated by Reversible Addition Fragmentation Chain Transfer (Raft) Polymerization. *Macromolecules* **2005**, *38* (6), 2131−2136.
(41) Chen, L.; Simpson, J. D.; Fuchs, A. V.; Rolfe, B. E.; Thurecht, K. J. Effects of Surface Charge of Hyperbranched Polymers on Cytotoxicity, Dynamic Cellular Uptake and Localization, Hemotoxicity, and Pharmacokinetics in Mice. *Mol. Pharmaceutics* **2017**, *14* (12), 4485−4497.
(42) Zhao, Y. M.; Houston, Z. H.; Simpson, J. D.; Chen, L. Y.; Fletcher, N. L.; Fuchs, A. V.; Blakey, I.; Thurecht, K. J. Using Peptide Aptamer Targeted Polymers as a Model Nanomedicine for Investigating Drug Distribution in Cancer Nanotheranostics. *Mol. Pharmaceutics* **2017**, *14* (10), 3539−3549.
(43) Pearce, A. K.; Simpson, J. D.; Fletcher, N. L.; Houston, Z. H.; Fuchs, A. V.; Russell, P. J.; Whittaker, A. K.; Thurecht, K. J. Localised Delivery of Doxorubicin to Prostate Cancer Cells through a Psma-Targeted Hyperbranched Polymer Theranostic. *Biomaterials* **2017**, *141*, 330−339.
(44) Fuchs, A. V.; Gemmell, A. C.; Thurecht, K. J. Utilising Polymers to Understand Diseases: Advanced Molecular Imaging Agents. *Polym. Chem.* **2015**, *6* (6), 868−880.
(45) Liu, Y.; Tseng, Y. C.; Huang, L. Biodistribution Studies of Nanoparticles Using Fluorescence Imaging: A Qualitative or Quantitative Method? *Pharm. Res.* **2012**, *29* (12), 3273−3277.
(46) Li, Y.; Boraschi, D. Endotoxin Contamination: A Key Element in the Interpretation of Nanosafety Studies. *Nanomedicine* **2016**, *11* (3), 269−287.
(47) Daneshian, M.; Guenther, A.; Wendel, A.; Hartung, T.; von Aulock, S. In Vitro Pyrogen Test for Toxic or Immunomodulatory Drugs. *J. Immunol. Methods* **2006**, *313* (1−2), 169−175.
(48) Gryshchuk, V.; Galagan, N. Silica Nanoparticles Effects on Blood Coagulation Proteins and Platelets. *Biochem. Res. Int.* **2016**, *2016*, 1−6.
(49) Gorbet, M. B.; Sefton, M. V. Biomaterial-Associated Thrombosis: Roles of Coagulation Factors, Complement, Platelets and Leukocytes. *Biomaterials* **2004**, *25* (26), 5681−5703.
(50) Vogler, E. A.; Siedlecki, C. A. Contact Activation of Blood-Plasma Coagulation. *Biomaterials* **2009**, *30* (10), 1857−1869.
(51) Oslakovic, C.; Cedervall, T.; Linse, S.; Dahlback, B. Polystyrene Nanoparticles Affecting Blood Coagulation. *Nanomedicine* **2012**, *8* (6), 981−986.
(52) Ilinskaya, A. N.; Dobrovolskaia, M. A. Nanoparticles and the Blood Coagulation System. Part I: Benefits of Nanotechnology. *Nanomedicine* **2013**, *8* (5), 773−784.
(53) Fischer, M.; Sperling, C.; Werner, C. Synergistic Effect of Hydrophobic and Anionic Surface Groups Triggers Blood Coagulation in Vitro. *J. Mater. Sci.: Mater. Med.* **2010**, *21* (3), 931−937.
(54) Michelson, A. D.; Barnard, M. R.; Krueger, L. A.; Valeri, C. R.; Furman, M. I. Circulating Monocyte-Platelet Aggregates Are a More Sensitive Marker of in Vivo Platelet Activation Than Platelet Surface P-Selectin: Studies in Baboons, Human Coronary Intervention, and Human Acute Myocardial Infarction. *Circulation* **2001**, *104* (13), 1533−1537.
(55) Kainthan, R. K.; Hester, S. R.; Levin, E.; Devine, D. V.; Brooks, D. E. In Vitro Biological Evaluation of High Molecular Weight Hyperbranched Polyglycerols. *Biomaterials* **2007**, *28* (31), 4581−4590.
(56) Selders, G. S.; Fetz, A. E.; Radic, M. Z.; Bowlin, G. L. An Overview of the Role of Neutrophils in Innate Immunity, Inflammation and Host-Biomaterial Integration. *Regen Biomater* **2017**, *4* (1), 55−68.
(57) Sperling, C.; Fischer, M.; Maitz, M. F.; Werner, C. Neutrophil Extracellular Trap Formation Upon Exposure of Hydrophobic Materials to Human Whole Blood Causes Thrombogenic Reactions. *Biomater. Sci.* **2017**, *5* (10), 1998−2008.
(58) Liz, R.; Simard, J. C.; Leonardi, L. B.; Girard, D. Silver Nanoparticles Rapidly Induce Atypical Human Neutrophil Cell Death by a Process Involving Inflammatory Caspases and Reactive Oxygen Species and Induce Neutrophil Extracellular Traps Release Upon Cell Adhesion. *Int. Immunopharmacol.* **2015**, *28* (1), 616−625.
(59) Fleischer, C. C.; Payne, C. K. Nanoparticle-Cell Interactions: Molecular Structure of the Protein Corona and Cellular Outcomes. *Acc. Chem. Res.* **2014**, *47* (8), 2651−2659.
(60) Gustafson, H. H.; Holt-Casper, D.; Grainger, D. W.; Ghandehari, H. Nanoparticle Uptake: The Phagocyte Problem. *Nano Today* **2015**, *10* (4), 487−510.
(61) Glass, J. J.; Kent, S. J.; De Rose, R. Enhancing Dendritic Cell Activation and Hiv Vaccine Effectiveness through Nanoparticle Vaccination. *Expert Rev. Vaccines* **2016**, *15* (3), 719−729.
(62) Ziegler-Heitbrock, L.; Ancuta, P.; Crowe, S.; Dalod, M.; Grau, V.; Hart, D. N.; Leenen, P. J.; Liu, Y.-J.; MacPherson, G.; Randolph, G. J.; et al. Nomenclature of Monocytes and Dendritic Cells in Blood. *Blood* **2010**, *116* (16), e74−e80.
(63) Peek, L. J.; Middaugh, C. R.; Berkland, C. Nanotechnology in Vaccine Delivery. *Adv. Drug Delivery Rev.* **2008**, *60* (8), 915−928.
(64) Coffman, R. L.; Sher, A.; Seder, R. A. Vaccine Adjuvants: Putting Innate Immunity to Work. *Immunity* **2010**, *33* (4), 492−503.
(65) Schroder, K.; Hertzog, P. J.; Ravasi, T.; Hume, D. A. Interferon-Γ: An Overview of Signals, Mechanisms and Functions. *J. Leukocyte Biol.* **2004**, *75* (2), 163−189.
(66) Schönbeck, U.; Libby, P. The Cd40/Cd154 Receptor/Ligand Dyad. *Cell. Mol. Life Sci.* **2001**, *58* (1), 4−43.
(67) Coles, D. J.; Rolfe, B. E.; Boase, N. R.; Veedu, R. N.; Thurecht, K. J. Aptamer-Targeted Hyperbranched Polymers: Towards Greater Specificity for Tumours in Vivo. *Chem. Commun. (Cambridge, U. K.)* **2013**, *49* (37), 3836−3838.
(68) Weissleder, R.; Nahrendorf, M.; Pittet, M. J. Imaging Macrophages with Nanoparticles. *Nat. Mater.* **2014**, *13* (2), 125−138.
(69) Frohlich, E. The Role of Surface Charge in Cellular Uptake and Cytotoxicity of Medical Nanoparticles. *Int. J. Nanomed.* **2012**, *7*, 5577−5591.
(70) Shannahan, J. H.; Bai, W.; Brown, J. M. Implications of Scavenger Receptors in the Safe Development of Nanotherapeutics. *Receptors Clin. Investig.* **2015**, *2* (3), e811.

DOI: 10.1021/acsabm.8b00220
ACS Appl. Bio Mater. 2018, 1, 756−767